HHS Public Access

Author manuscript

Nature. Author manuscript; available in PMC 2013 February 16.

Published in final edited form as:

Nature. 2012 August 16; 488(7411): 389–393. doi:10.1038/nature11250.

NLRP6 Negatively Regulates Innate Immunity and Host Defense Against Bacterial Pathogens

Paras K. Anand[1], **R. K. Subbarao Malireddi**[1], **John R. Lukens**[1], **Peter Vogel**[2], **John Bertin**[3], **Mohamed Lamkanfi**[4,5,6], and **Thirumala-Devi Kanneganti**[1,6,*]

[1]Department of Immunology, St. Jude Children's Research Hospital, Memphis, TN, 38105, USA

[2]Animal Resources Center and the Veterinary Pathology Core, St. Jude Children's Research Hospital, Memphis, TN, 38105, USA

[3]Pattern Recognition Receptor DPU, Immuno-Inflammation TA, GlaxoSmithKline, Collegeville, PA, 19426, USA

[4]Department of Biochemistry, Ghent University, B-9000 Ghent, Belgium

[5]Department of Medical Protein Research, VIB, B-9000 Ghent, Belgium.

Abstract

Members of the intracellular nucleotide-binding and oligomerization domain (NOD)-like receptor (NLR) family contribute to immune responses through activation of NF-κB, type I interferon and inflammasome signaling[1]. Mice lacking the NLR family member NLRP6 were recently shown to be susceptible to colitis and colorectal tumorigenesis[2-4], but the role of NLRP6 in microbial infections and the nature of the inflammatory signaling pathways regulated by NLRP6 remain unclear. Here, we show that *Nlrp6*-deficient mice were highly resistant to infection with the bacterial pathogens *Listeria monocytogenes*, *Salmonella typhimurium* and *Escherichia coli*. Infected *Nlrp6*-deficient mice had increased numbers of monocytes and neutrophils in circulation, and NLRP6 signaling in both hematopoietic and radio-resistant cells contributed to increased susceptibility. *Nlrp6*-deficiency enhanced activation of MAPK and canonical NF-κB upon TLR, but not cytosolic NOD1/2 ligation *in vitro*. Consequently, infected *Nlrp6*-deficient cells produced elevated levels of NF-κB- and MAPK-dependent cytokines and chemokines. Thus, our results reveal NLRP6 as a negative regulator of inflammatory signaling, and demonstrate a role for this NLR in impeding clearance of both Gram-positive and –negative bacterial pathogens.

[*]**Correspondence should be addressed to:** Thirumala-Devi Kanneganti Department of Immunology, St Jude Children's Research Hospital MS #351, 570, St. Jude Place, Suite E7004 Memphis TN 38105-2794 Tel: (901) 595-3634; Fax. (901) 595-5766. Thirumala-Devi.Kanneganti@StJude.org..

[6]Equal last author.

Author Contributions

T.-D.K., M.L., P.K.A. designed research; P.K.A., R.K.S.M. and J.R.L. performed the experiments; P.V. performed and analyzed the histopathology data; J.B. provided essential reagents; T.-D.K., M.L., P.K.A., R.K.S.M., J.R.L., P.V. and J.B. analyzed the data; P.K.A, M.L. and T.-D.K. wrote the paper; and T.-D.K. conceived of the study, designed the experiments and provided overall direction.

Keywords

NLRP6; NLR; *Listeria*; *Salmonella*; NF-kB; ERK

Despite the availability of antibiotics, bacterial infections continue to threaten public health worldwide. According to CDC estimates, roughly 48 million people in the Unites States get sick every year due to foodborne illnesses resulting in 3000 deaths annually[5]. *Listeria* and *Salmonella* belong to the top three pathogens contributing to foodborne infections resulting in death[5,6]. *Listeria monocytogenes* and *Salmonella typhimurium* are facultative intracellular pathogens that have the ability to survive and replicate within macrophages and dendritic cells. *Listeria* rapidly escapes the phagosome to replicate in the cytosol, whereas *Salmonella* lacks a phagosomal escape mechanism and inhabits the salmonella-containing vacuole (SCV)[7-9]. A deeper understanding of the mechanisms by which these and other bacterial pathogens are sensed by the immune system may contribute to new approaches for developing antimicrobials. Cells of the innate immune system detect micro-organisms by means of a limited set of evolutionary conserved pattern recognition receptors (PRRs)[10]. NLR proteins represent a family of intracellular PRRs that survey the cytoplasmic compartment for infectious agents and cellular damage[1]. NLRs such as NOD1 and NOD2 contribute to host defense against microbial pathogens by inducing the production of pro-inflammatory cytokines through activation of NF-κB and MAPK signaling, whereas NLRs such as NLRP1, NLRP3 and NLRC4 facilitate the activation of inflammatory caspases in large multi-protein complexes termed inflammasomes[11,12]. Our knowledge of the former NLRs has markedly improved in recent years, but initial characterization of NLRP6 has only recently been reported[2-4,13]. These studies demonstrated NLRP6 to contribute to protection against colitis, colorectal tumorigenesis and non-alcoholic steatosis by regulating the integrity of the epithelial barrier and by altering the composition of the gut microflora[2-4,13]. However, its role in host defense against microbial pathogens and the signaling pathways regulated by NLRP6 remain unclear.

To characterize NLRP6 expression in immune cells, *Nlrp6* transcript abundance in immune cells and epithelial cells was analyzed by real-time qPCR. As previously reported[14], neutrophils and T cells showed the highest expression levels for *Nlrp6*, followed by macrophages, epithelial cells and dendritic cells (**Fig. S1**), suggesting that NLRP6 may play an important role in these cell types. The domain architecture of NLRP6 resembles that of NLRP3 and consists of a N-terminal Pyrin domain, a centrally located nucleotide-binding domain and a stretch of C-terminally-located leucine rich repeats[1]. *Nlrp6*-deficient mice have been described[2-4,13], and animals appeared healthy and did not display gross abnormalities when housed in a specific-pathogen-free facility (data not shown). To characterize the role of NLRP6 during microbial infections, wildtype (WT) and *Nlrp6*$^{-/-}$ mice were infected intraperitoneally (i.p.) with a lethal dose of 10^6 CFU of *Listeria monocytogenes (L. monocytogenes)*. Whereas the entire cohort of WT mice succumbed to infection within 5-6 days, 75% of *Nlrp6*$^{-/-}$ mice survived the infection and were still alive at day 20 post-infection **(Fig. 1a)**. In agreement, WT mice lost on average 20% of their initial body weight before succumbing to infection, whereas weight loss in *Nlrp6*$^{-/-}$ mice was initially limited (<10% by day 3) and body weight gradually returned to normal levels after

day 4 **(Fig. 1b)**. To examine whether differential mortality in WT and *Nlrp6*$^{-/-}$ mice was associated with differences in bacterial dissemination, bacterial burdens in systemic organs was determined at days 1 and 3 post-infection. Notably, both liver and spleen of *Nlrp6*$^{-/-}$ mice contained significantly less bacteria than those of WT mice at day 1 (**Fig. 1c, d**); and this difference further increased by day 3 post-infection **(Fig. 1e, f)**. Immunohistochemical analysis of liver sections confirmed *L. monocytogenes* to be nearly absent from liver capsules of *Nlrp6*$^{-/-}$ mice, whereas those of WT mice were morphologically distorted due to high pathogen counts **(Fig. 1g)**. *L. monocytogenes* infection is known to trigger histopathological lesions and the formation of inflammatory cell foci, the size of which correlates with disease severity[15]. To examine the extent of immune cell infiltration, hematoxylin and eosin (H&E)-stained liver sections of *L. monocytogenes*-infected WT and *Nlrp6*$^{-/-}$ mice were compared. In agreement with our previous results, inflammatory cell foci in *Nlrp6*$^{-/-}$ livers were significantly smaller than those found in WT mice at day 3 post-infection **(Fig. 1h and Fig. S2)**. To examine the role of NLRP6 during alternative infection routes, cohorts of WT and *Nlrp6*$^{-/-}$ mice were infected with *L. monocytogenes* intravenously (i.v.). As with *i.p.*-infected animals (**Fig. 1e, f**), bacterial counts in the liver and spleen of *i.v.*-infected *Nlrp6*$^{-/-}$ mice were significantly lower than the burdens measured in WT mice at day 3 post-infection **(Fig. S3)**. *Nlrp6*$^{-/-}$ mice were recently shown to have an altered microflora composition that is transferable to co-housed WT mice[3]. In agreement, 16S rRNA analysis confirmed an increased abundance of Bacteroidetes (Prevotellaceae family) in the gastro-intestinal tract of *Nlrp6*$^{-/-}$ mice relative to the microbiota composition of separately housed WT mice **(Fig. S4a)**. Co-housing WT with *Nlrp6*$^{-/-}$ mice for 4 weeks equalized the prevalence of Prevotellaceae in WT and *Nlrp6*$^{-/-}$ mice **(Fig. S4a, b)**. However, co-housing did not alter the resistant phenotype of *Nlrp6*$^{-/-}$ mice to *L. monocytogenes* infection because *Nlrp6*$^{-/-}$ mice contained fewer bacteria in the spleen and liver compared to the levels of co-housed WT mice (**Fig. S4c, d**). These results suggest that NLRP6 regulates *L. monocytogenes* infection independently of its microflora composition.

To determine whether resistance of *Nlrp6*$^{-/-}$ mice to infection is specific to *L. monocytogenes* or extends to other pathogens, cohorts of WT and *Nlrp6*$^{-/-}$ mice were infected i.p with *Salmonella typhimurium (S. typhimurium)*. Resistance to *S. typhimurium* infection was increased in *Nlrp6*$^{-/-}$ mice as illustrated by the significantly lower bacterial burdens detected in the liver and spleen at days 1 (**Fig. 1i, j**) and 3 (**Fig. 1k, l**) post-infection. Inbred mice may carry distinct alleles of mouse *Nramp1* (natural resistance-associated macrophage protein one), the gene products of which may differentially regulate host resistance to *Salmonella* and other bacterial pathogens[16]. Nramp1 transcripts of both *Nlrp6*$^{-/-}$ *and* wildtype (C57BL/6J) mice encoded the NRAMP1 Gly/Asp$_{169}$ polymorphism (data not shown), ruling out a possible impact on the increased resistance of *Nlrp6*$^{-/-}$ mice to *Salmonella* infection. Because both *S. typhimurium* and *L. monocytogenes* are facultative intracellular pathogens, we determined whether NLRP6 modulated resistance against extracellular pathogens such as *Escherichia coli* (*E. coli*) as well. To this end, we analyzed CFUs in systemic organs of wildtype and *Nlrp6*$^{-/-}$ mice 2 days after infection with this Gram-negative extracellular pathogen. Notably, bacterial burdens in the liver and spleen of *Nlrp6*$^{-/-}$ mice were significantly lower than in wildtype mice (**Fig. S5**). Together, these results suggest that NLRP6 may promote systemic dissemination and growth of both Gram-

negative and -positive (*S. typhimurium* and *L. monocytogenes*, respectively) as well as intracellular and extracellular bacteria (*S. typhimurium* and *E. coli*, respectively) in infected hosts.

Myeloid cells play critical roles in early host defense responses against microbial pathogens. They develop in the bone marrow, but egress into circulation upon infection[17]. Because *Nlrp6* is expressed in monocytes and neutrophils (**Fig. S1**), we initially made use of an automated haematology analyzer - which determines blood cell types based on morphology - to characterize the influx of monocytes and neutrophils in peripheral blood of WT and *Nlrp6*$^{-/-}$ mice. Prior to infection, monocyte and neutrophil precursors in the bone marrow were similar (**Fig. S6**), and no significant differences in counts of circulating monocytes and neutrophils were noted in naïve WT and *Nlrp6*$^{-/-}$ mice (**Fig. S7**), suggesting that basal differentiation of myeloid progenitor cells was not affected in these mice. However, both the fraction and total cell counts of circulating monocytes and neutrophils were markedly higher in peripheral blood of *L. monocytogenes*-infected *Nlrp6*$^{-/-}$ mice (**Fig. 2a,b**). To confirm these results, immune cell infiltration in the peritoneal cavity of *L. monocytogenes*-infected animals was analyzed by flow cytometry. Basal monocyte and neutrophil populations in the peritoneal cavity of naïve WT and *Nlrp6*$^{-/-}$ mice did not differ (data not shown). In contrast, significantly higher infiltration of monocytes and neutrophils was observed in the peritoneal cavity of *L. monocytogenes*-infected *Nlrp6*$^{-/-}$ mice over WT mice **(Fig. 2c, d and Fig. S8a,b)**. Unlike granulocyte populations, the numbers of circulating lymphocytes and infiltrated T-cells in the peritoneal cavity were similar in *L. monocytogenes*-infected WT and *Nlrp6*$^{-/-}$ mice **(Fig. S8c,d)**. Concurrently, *Nlrp6*-deficiency did not alter the induction of T-cell responses because the frequency and number of OVA-specific CD8^{+} T-cells were similar in WT and *Nlrp6*$^{-/-}$ mice that were infected with OVA-expressing *Listeria* (Lm-OVA) **(Fig. S9)**. Taken together, these results suggest NLRP6 to inhibit the influx of monocytes and neutrophils in circulation and into the peritoneum during bacterial infections.

To further examine the cell types responsible for NLRP6-mediated dissemination of bacterial infections, we created WT and *Nlrp6*$^{-/-}$ bone marrow chimeras. Bone marrow reconstitution was confirmed to reach a level of approximately 95% in irradiated mice (data not shown). As expected, *Nlrp6*$^{-/-}$ mice that were transplanted with *Nlrp6*$^{-/-}$ bone marrow were more resistant to *L. monocytogenes* infection than WT mice receiving WT bone marrow (**Fig. 2e-g**). Notably, both WT mice transplanted with *Nlrp6*$^{-/-}$ bone marrow and *Nlrp6*$^{-/-}$ mice that received WT bone marrow showed an intermediate level of protection against *L. monocytogenes* **(Fig. 2e-g)**. Indeed, weight loss (**Fig. 2e**) and bacterial dissemination to the spleen and liver (**Fig. 2f, g**) of these two chimera groups was in between the levels seen for the two control groups **(Fig. 2e-g)**. These results suggest that both hematopoietic and non-hematopoietic cells contribute to NLRP6-mediated inhibition of bacterial clearance.

To gain understanding of the signaling mechanisms by which NLRP6 regulates bacterial infections, we first examined bacterial clearance by *in vitro* cultured *Nlrp6*$^{-/-}$ macrophages. Phagocytosis and bacterial replication of *L. monocytogenes* in *Nlrp6*$^{-/-}$ bone-marrow derived macrophages (BMDMs) were comparable to those of WT macrophages (**Fig. S10**). Unlike results from overexpression studies[14], but in agreement with a recent report that employed

Nlrp6 siRNA knockdown in human PBMCs[18], we found NLRP6 to be dispensable for inflammasome activation by *L. monocytogenes* and *S. typhimurium* because neither caspase-1 processing nor maturation of IL-1β were affected in *Nlrp6*-deficient macrophages infected with these pathogens or stimulated with the bacterial ligands LPS and Pam3-CSK4 in the presence of ATP (**Fig. S11**).

We next assessed the potential role of NLRP6 in regulating activation of NF-κB and MAP kinase signaling in macrophages infected with *L. monocytogenes*. In WT BMDMs, phosphorylation of ERK1/2 and IκB peaked 60 min post-infection and gradually diminished thereafter (**Fig. 3a, b**). Infected *Nlrp6*$^{-/-}$ macrophages had significantly increased phospo-ERK1/2 levels, and failed to down-regulate phospho-IκB (**Fig. 3a, b**). In addition to macrophages, *Nlrp6*$^{-/-}$ neutrophils also responded to *L. monocytogenes* infection with elevated phospho-IκB and phospo-ERK1/2 levels (**Fig. S12a**), suggesting that NLRP6 may negatively regulate NF-κB and ERK activation downstream of TLRs. In agreement, the TLR2 ligand Pam3CSK4 also induced increased phospo-ERK1/2 and phospho-IκB levels in *Nlrp6*$^{-/-}$ BMDMs (**Fig. 3c, d**). Similar observations were made using the TLR4 ligand LPS (**Fig. 3e, f**). Increased phospho-IkB and phospho-ERK1/2 levels were also noted in liver lysates of infected *Nlrp6*$^{-/-}$ mice (**Fig. 3g, h**). Unlike with TLR agonists, phospho-IkB and phospho-ERK1/2 levels induced upon ligation of the cytosolic receptors NOD1 and NOD2 were similar in WT and *Nlrp6*$^{-/-}$ cells (**Fig. S12b,c**), suggesting NLRP6 to be specifically involved in negatively regulating TLR-induced NF-κB and MAP kinase activation. Thus, in marked contrast to overexpression studies[14], our results in *Nlrp6*$^{-/-}$ cells suggest that NLRP6 may diminish rather than enhance TLR-induced activation of NF-κB and ERK signalling. To further confirm the role of NLRP6 in regulating these pathways, we measured the production of NF-κB- and MAP-kinase-dependent cytokine and chemokine levels at different time points. Abundance of TNFα, IL-6 and KC transcripts in cell lysates and secreted cytokines in culture supernatants were significantly higher in *Nlrp6*$^{-/-}$ macrophages infected with *L. monocytogenes*, or stimulated with Pam3CSK4 and LPS (**Fig. S13a-d**). Interferon-β transcript levels nearly doubled in LPS-stimulated *Nlrp6*$^{-/-}$ macrophages after 2 h stimulation, but subsequently returned to levels of WT cells **(Fig. S14)**. Cytotoxicity was limited to baseline levels in both WT and *Nlrp6*$^{-/}$ macrophages, ruling out an important role for cell death induction in differential secretion of cytokines and chemokines **(Fig. S15)**. Increased levels of IL-6 and KC were also measured in serum and the peritoneal cavity of infected *Nlrp6*$^{-/-}$ mice **(Fig. S13e, f)**. These results suggest that NLRP6 specifically suppresses TLR-induced NF-κB and MAP-kinase activation during *L. monocytogenes* infection *in vitro* and *in vivo*.

NF-κB is a family of nuclear transcriptional regulators that initiate pro-inflammatory gene expression[19]. To determine whether canonical or non-canonical NF-κB activation is altered in *Nlrp6*$^{-/-}$ deficient cells, we analyzed the phosphorylation status of the non-canonical NF-κB effector p100, whereas p105 phosphorylation status was monitored as a parameter of canonical NF-κB signaling. *L. monocytogenes* infection induced significantly higher levels of phosphorylated p105 in *Nlrp6*$^{-/-}$ macrophages, whereas those of phosphorylated p100 were similar in WT and *Nlrp6*-deficient macrophages (**Fig. 4a**). Similar results were obtained when analyzing the isolated cytosolic fraction of *L. monocytogenes*-infected cells

(**Fig. 4a**). Additionally, this correlated with increased translocation of RelA in the nuclear fraction of infected *Nlrp6*-deficient cells, whereas the levels of the non-canonical effector RelB were similar in WT and *Nlrp6*$^{-/-}$ macrophages (**Fig. 4a**). Confocal immunofluorescence microscopy of *L. monocytogenes*-infected WT and *Nlrp6*$^{-/-}$ cells confirmed the increased nuclear translocation of RelA in the latter genotype (**Fig. 4b, c**). Increased p105 phosphorylation was also evident in total and cytosolic lysates of Pam3CSK4-stimulated *Nlrp6*$^{-/-}$ macrophages (**Fig. 4d**). In addition, enhanced RelA translocation was confirmed by Western blotting in nuclear lysates and by confocal immunofluorescence staining (**Fig. 4d-f**). qPCR analysis of IRAK-M and A20 failed to demonstrate differential expression of these negative regulators of TLR signaling in LPS- and Pam3CSK4-stimulated *Nlrp6*-deficient cells **(Fig. S16)**. Although further analysis is required to determine the precise level at which NLRP6 negatively regulates TLR-induced responses, our results indicate that NLRP6 suppresses TLR-induced MAP kinase and canonical NF-κB signaling to dampen the production of pro-inflammatory cytokines and chemokines during bacterial infection. NLRP6 activation consequently leads to increased susceptibility to both intracellular (*L. monocytogenes* and *S. typhimurium*) and extracellular (*E. coli*) as well as Gram-positive (*L. monocytogenes*) and –negative (*E. coli* and *S. typhimurium*) bacterial pathogens. Our bone-marrow chimera experiments suggested both the hematopoietic and non-hematopoietic compartments to contribute to the increased resistance to infection of *Nlrp6*$^{-/-}$ mice. We further demonstrated here that NLRP6 plays a critical role in regulating host and immune responses in cells of the myeloid lineage, and further analysis is required to determine the specific non-hematopoietic cell type(s) contributing to NLRP6-mediated host defense signaling *in vivo*.

The detrimental role of NLRP6 during systemic infection with bacterial pathogens appears in sharp contrast with its protective role in gastro-intestinal tract, where it contributes to maintaining a healthy composition of the gut microbiota[20]. We hypothesize that these apparently contradictory roles of NLRP6 may be explained by the spatiotemporal context in which it operates. As NLRP6 appears critical for dampening the production of pro-inflammatory cytokines and chemokines downstream of TLRs, it may play a protective role under conditions where strong inflammatory responses might be detrimental to the host (as during colitis). On the other hand, NLRP6 may play an adverse role during bacterial infections and other situations in which potent inflammatory responses would be protective to the host.

Notably, previous studies characterizing the NLR family members NOD1, NOD2, NLRC4 and NLRP3 all pointed to a protective role for these NLRs in clearing microbial pathogens, and deficiency in these NLRs led to increased morbidity and mortality in infected animals[21-24]. In contrast, our data suggest NLRP6 to dampen inflammatory signaling, thereby promoting bacterial dissemination and colonization of systemic organs of the host. In light of these findings, we propose that one subclass of NLRs (including NOD1, NOD2 and NLRC4) may directly respond to microbial pathogens detected in intracellular compartments by initiating pro-inflammatory signaling that eventually contributes to bacterial clearance. A second subclass of NLR proteins, such as NLRP6, may act as a molecular switch to dampen or silence TLR–induced pathways triggered by extracellular

recognition of bacterial ligands to prevent overt pathology. Regardless, our results highlight a critical role for NLRP6 in dampening host responses against several bacterial pathogens and suggest that therapeutic inhibition of NLRP6 activation may prove beneficial for treating infectious diseases.

Methods Summary

Nlrp6 knock-out mice were generated as described previously[2-4,13]. *In vivo* infection experiments were done on female mice that were 8-12 weeks old and were conducted under protocols approved by St. Jude Children's Research Hospital Committee on Use and Care of Animals. Lethal *L. monocytogenes* infection was established by infecting female mice with 1×10^6 CFU bacteria administered intraperitoneally (i.p). To study bacterial clearance, mice were infected with *L. monocytogenes* either at a dose of 3×10^5 CFU (i.p.). Immune cell infiltration in the circulation of infected mice was performed on blood collected by submandibular venipuncture and analyzed on a Forcyte hematology analyzer. Bone-marrow chimera experiment was done as described previously. Bone-marrow macrophages were prepared and infected as described previously. Samples were run on SDS-PAGE and immunoblotted with antibodies as reported previously. Data are expressed as mean ± s.e.m. Differences were analyzed by Student't t-test. *P* values ≤ 0.05 were considered significant.

METHODS

Bacterial infections and enumeration of bacterial burdens

Lethal *L. monocytogenes* infection was established by infecting female mice with 1×10^6 CFU bacteria administered intraperitoneally (i.p). Animals were weighed and monitored daily for mortality for up to 20 days. Differences in survival were analyzed by Mantel-Cox test. To study bacterial clearance, mice were infected with *L. monocytogenes* either at a dose of 3×10^5 CFU (i.p.) or at 3×10^4 CFU (i.v.)[7]. Alternatively, mice were infected with *S. typhimurium* at a dose of 1×10^4 CFU (i.p). E. Coli infection was performed in 6 weeks old female mice with 5×10^7 CFU (i.p.). Mice were sacrificed at days 1 and 3 post-infection (or day 2 in case of *E. Coli* infection), liver and spleen tissue was homogenized and bacterial burdens were enumerated by serial dilution on Brain-Heart-Infusion agar or LB agar plates as described previously[7].

Histopathology

Formalin-preserved liver sections were processed and embedded in paraffin by standard techniques. Longitudinal sections of 5 μm thick were stained with hematoxylin and eosin (H&E) and examined by a pathologist blinded to the experimental groups. For immunohistochemistry, formalin-fixed paraffin-embedded tissues were cut into 4 μm sections and slides were stained with anti-*Listeria* antibody.

Analysis of immune cell infiltration in the peritoneum and in circulation

WT and *Nlrp6*$^{-/-}$ female mice were infected with 3×10^5 *L. monocytogenes* (i.p.). At 3h post-infection, blood was collected by submandibular venipuncture and analyzed on a Forcyte hematology analyzer (Oxford Sciences) by a hematologist blinded to the

experimental groups. In addition, cells were collected by peritoneal lavage in either 1m of IMDM (for cytokines analysis) or in 10 ml IMDM (for total cell recruitment to the cavity) on ice. Cells obtained from WT and *Nlrp6*$^{-/-}$ mice were washed twice with PBS and surface-stained for anti-CD11b (Biolegend; clone # M1/70), anti-Gr-1 (Biolegend; clone # RB6-8C5), anti-TCR β (Biolegend; clone # H57-597) and anti-Ly6G (BD Biosciences). Monocytes were characterized as CD11b^{+}Gr-1^{-}TCRb^{-} cells, whereas CD11b^{+}Gr1^{+} cells were taken as neutrophils.

WT and *Nlrp6*$^{-/-}$ mice were intravenously infected with 3×10^{4} colony forming units (CFUs) of *Listeria monocytogenes* that was engineered to express the OVA antigen (LmOVA). At the peak of the T cell response (day 8), 100 μl of peripheral blood was obtained and peripheral blood leukocytes (PBLs) were isolated following red blood cell lysis. Cells were FACs stained with OVA-tetramers and T cell lineage markers (anti-CD4 and anti-CD8).

Bone-marrow chimeras

Bone marrow transfer was used to create *Nlrp6*$^{-/-}$ chimera mice wherein the genetic deficiency of Nlrp6 was contained to either the circulating cells (*Nlrp6*$^{-/-}$ > WT chimera) or non-hematopoietic tissue (WT > *Nlrp6*$^{-/-}$). Briefly, bone-marrow cells were collected from the femur and tibia of congenic WT (expressing CD45.1 leukocyte antigen) or *Nlrp6*$^{-/-}$ (expressing CD45.2 leukocyte antigen) donor mice by flushing with HBSS. After thorough washing, cells were resuspended in PBS and 100ul of this cell suspension containing 10^{7} cells was injected retro-orbitally to the irradiated host mice. Four chimera groups were generated (WT > WT; WT > *Nlrp6*$^{-/-}$; *Nlrp6*$^{-/-}$ > WT and *Nlrp6*$^{-/-}$ > *Nlrp6*$^{-/-}$). The use of CD45.1 expressing congenic WT mice facilitated the verification of bone-marrow reconstitution at 6 weeks after irradiation. Cells in the blood were labelled with APC-conjugated CD45.1 and FITC-conjugated CD45.2 antibody. The chimera mice had ~95% reconstitution with the donor bone-marrow.

Macrophage culture and in vitro stimulation

BMDMs and peritoneal macrophages were prepared as described previously[7]. Cells were subsequently infected with *L. monocytogenes or S. typhimurium* as indicated; or stimulated with Pam3-CSK4 (10 μg/ml) or LPS (100 ng/ml). At the indicated time points, supernatant was collected and stored at -80°C for cytokine analysis at a later time and cells were lysed in RIPA buffer supplemented with complete protease inhibitor cocktail (Roche) and PhosSTOP (Roche). For analysis of caspase-1 activation and IL-1β secretion, macrophages were cultured with bacteria or TLR ligands for 3 h followed by addition of 5 mM ATP (Sigma) for 30 min.

In vivo lysates and serum cytokines

Liver was obtained from control and infected WT and *Nlrp6*$^{-/-}$ mice at 3h post-infection. The tissue was homogenized in RIPA buffer supplemented with complete protease inhibitor cocktail (Roche) and PhosSTOP (Roche). At this time, blood was also collected by submandibular venipuncture for serum cytokine analysis.

ELISA

Cytokine ELISA was performed according to manufacturer's instructions (Milliplex).

LDH assay

LDH assay was performed by using Promega cytotoxicity kit according to manufacturer's instructions.

Western blotting

Lysates were prepared in RIPA buffer supplemented with complete protease inhibitor cocktail (Roche) and PhosSTOP (Roche). Samples were resolved by SDS-PAGE and transferred to PVDF membranes by electroblotting. Membranes were blocked in 5% nonfat milk and incubated overnight with primary antibodies at 4°C and subsequently with HRP-tagged secondary antibodies at room temperature for 1h. Immunoreactive proteins were visualized with ECL method (Pierce). Semi-quantitative analysis of WB bands was performed by Image J program.

Confocal Immunofluorescence microscopy

Cells were grown overnight on glass coverslips. Next day, WT and *Nlrp6*$^{-/-}$ macrophages were either infected with GFP-labeled *L. monocytogenes* or stimulated with Pam3. The cells were fixed with 4% paraformaldehyde and processed for microscopy with anti-RelA antibody (Santa-Cruz) as described previously[7]. Cells, grown on coverslips, were mounted on glass slides with ProLong gold antifade reagent (Invitrogen) and visualized with a Nikon C1 confocal microscope using 40X objective lens. The images were processed and analyzed with Image J program.

Real-time PCR

Total RNA was isolated with Trizol (Invitrogen) according to the manufacturer's instructions. For Nlrp6 expression, macrophages and dendritic cells were differentiated from bone-marrow cells, neutrophils were obtained from the peritoneal cavity after 5h of thioglycollate injection, T-cells were purified from the spleen and epithelial cells were isolated from the intestine. 1 μg of RNA was reverse-transcribed to cDNA with poly dT primers using First-strand cDNA synthesis kit (Invitrogen). Transcript levels of different genes were analyzed using SYBR-Green (Applied Biosystems) on an ABI7500 real-time PCR instrument. Expression of GAPDH was used as an internal control. mRNA expression levels were normalized against a standard curve.

Co-housing experiments and analysis of fecal flora

Age and gender matched WT and *Nlrp6*$^{-/-}$ mice were coused together at 1:1 ratio for four weeks as described previously[3]. Fecal samples were obtained from the two groups of mice before and after co-housing. Frozen fecal samples were processed for DNA isolation using QiaAmp stool kit (Qiagen). 10ng of DNA was used in the PCR reaction and previously reported primer pairs were used for analysis of 16S rRNA analysis[3].

Intracellular growth curve

WT and *Nlrp6*$^{-/-}$ macrophages were infected with *L. monocytogenes* with a moi of 1:1 and intracellular growth curves were generated as described previously[25].

Nramp1 genotyping

A fragment of the Nramp1 gene was amplified by PCR using primers 5′-GCCATTGTGGGCTCAGATATGC-3′ and 5′-GCCATTATGGTAATGAGGAGACCG. The resulting PCR fragment was purifed and sequenced using the primer 5′-GCCATTGTGGGCTCAGATATGC-3′.

Statistics

Differences in the survival of animals were calculated by log-rank Mantel-Cox test using Graphpad Prism software. In all other experiments, p values were calculated using the two-tailed Student's t-test. p-values are denoted by *p<0.05, **p<0.01, ***p<0.001, ****p<0.0001.

Supplementary Material

Refer to Web version on PubMed Central for supplementary material.

Acknowledgements

We thank Drs. Anthony Coyle, Ethan Grant and Richard Flavell (Yale University) for generous supply of mutant mice. ML is supported by grants from the European Union Framework Program 7 (Marie-Curie Grant 256432), European Research Council (grant 281600) and the Fund for Scientific Research Flanders (G030212N, 1.2.201.10.N.00 and 1.5.122.11.N.00). This work was supported by National Institute of Health Grants (R01AR056296), and the American Lebanese Syrian Associated Charities (ALSAC) to T.-D.K.

Abbreviations

NLR	NOD-like receptor
TLR	Toll-like receptor
WT	wild-type

References

1. Kanneganti TD, Lamkanfi M, Nunez G. Intracellular NOD-like receptors in host defense and disease. Immunity. 2007; 27:549–559. [PubMed: 17967410]
2. Chen GY, Liu M, Wang F, Bertin J, Nunez G. A functional role for Nlrp6 in intestinal inflammation and tumorigenesis. J Immunol. 2011; 186:7187–7194. [PubMed: 21543645]
3. Elinav E, et al. NLRP6 inflammasome regulates colonic microbial ecology and risk for colitis. Cell. 2011; 145:745–757. [PubMed: 21565393]
4. Normand S, et al. Nod-like receptor pyrin domain-containing protein 6 (NLRP6) controls epithelial self-renewal and colorectal carcinogenesis upon injury. Proc Natl Acad Sci U S A. 2011; 108:9601–9606. [PubMed: 21593405]
5. CDC. 2010. http://www.cdc.gov/foodborneburden/2011-foodborne-estimates.html
6. Scallan E, et al. Foodborne illness acquired in the United States--major pathogens. Emerg Infect Dis. 2011; 17:7–15. [PubMed: 21192848]

7. Anand PK, et al. TLR2 and RIP2 pathways mediate autophagy of Listeria monocytogenes via ERK activation. J Biol Chem. 2011; 286:42981–42991. [PubMed: 22033934]
8. Corr SC, O'Neill LA. Listeria monocytogenes infection in the face of innate immunity. Cell Microbiol. 2009; 11:703–709. [PubMed: 19191786]
9. Hybiske K, Stephens RS. Exit strategies of intracellular pathogens. Nat Rev Microbiol. 2008; 6:99–110. [PubMed: 18197167]
10. Creagh EM, O'Neill LA. TLRs, NLRs and RLRs: a trinity of pathogen sensors that co-operate in innate immunity. Trends Immunol. 2006; 27:352–357. [PubMed: 16807108]
11. Kanneganti TD. Central roles of NLRs and inflammasomes in viral infection. Nat Rev Immunol. 2010; 10:688–698. [PubMed: 20847744]
12. Petrilli V, Dostert C, Muruve DA, Tschopp J. The inflammasome: a danger sensing complex triggering innate immunity. Curr Opin Immunol. 2007; 19:615–622. [PubMed: 17977705]
13. Henao-Mejia J, et al. Inflammasome-mediated dysbiosis regulates progression of NAFLD and obesity. Nature. 2012; 482:179–185. [PubMed: 22297845]
14. Grenier JM, et al. Functional screening of five PYPAF family members identifies PYPAF5 as a novel regulator of NF-kappaB and caspase-1. FEBS Lett. 2002; 530:73–78. [PubMed: 12387869]
15. Stevenson MM, Kongshavn PA, Skamene E. Genetic linkage of resistance to Listeria monocytogenes with macrophage inflammatory responses. J Immunol. 1981; 127:402–407. [PubMed: 7252146]
16. Lara-Tejero M, et al. Role of the caspase-1 inflammasome in Salmonella typhimurium pathogenesis. J Exp Med. 2006; 203:1407–1412. [PubMed: 16717117]
17. Serbina NV, Pamer EG. Monocyte emigration from bone marrow during bacterial infection requires signals mediated by chemokine receptor CCR2. Nat Immunol. 2006; 7:311–317. [PubMed: 16462739]
18. Meixenberger K, et al. Listeria monocytogenes-infected human peripheral blood mononuclear cells produce IL-1beta, depending on listeriolysin O and NLRP3. J Immunol. 2010; 184:922–930. [PubMed: 20008285]
19. Waterfield MR, Zhang M, Norman LP, Sun SC. NF-kappaB1/p105 regulates lipopolysaccharide-stimulated MAP kinase signaling by governing the stability and function of the Tpl2 kinase. Mol Cell. 2003; 11:685–694. [PubMed: 12667451]
20. van Ooij C. Immunology: NLRP6 keeps the bad bacteria at bay. Nat Rev Microbiol. 2011; 9:481. [PubMed: 21625246]
21. Girardin SE, et al. Nod1 detects a unique muropeptide from gram-negative bacterial peptidoglycan. Science. 2003; 300:1584–1587. [PubMed: 12791997]
22. Kobayashi KS, et al. Nod2-dependent regulation of innate and adaptive immunity in the intestinal tract. Science. 2005; 307:731–734. [PubMed: 15692051]
23. Franchi L, et al. Cytosolic flagellin requires Ipaf for activation of caspase-1 and interleukin 1beta in salmonella-infected macrophages. Nat Immunol. 2006; 7:576–582. [PubMed: 16648852]
24. Broz P, et al. Redundant roles for inflammasome receptors NLRP3 and NLRC4 in host defense against Salmonella. J Exp Med. 2010; 207:1745–1755. [PubMed: 20603313]
25. Portnoy DA, Jacks PS, Hinrichs DJ. Role of hemolysin for the intracellular growth of Listeria monocytogenes. J Exp Med. 1988; 167:1459–1471. [PubMed: 2833557]

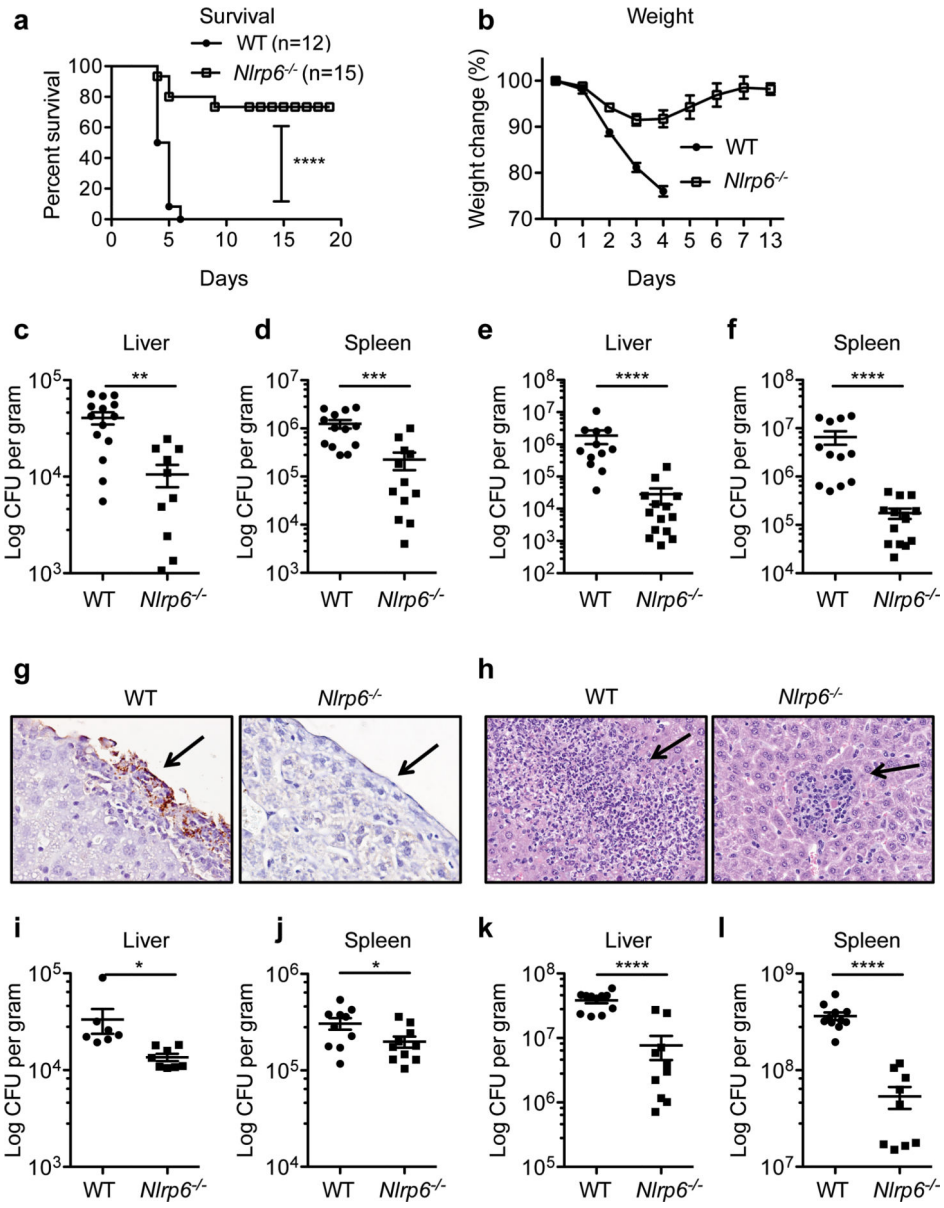

Figure 1. *Nlrp6*$^{-/-}$ mice are resistant to *Listeria and Salmonella* infection

a), WT and *Nlrp6*$^{-/-}$ mice were infected i.p. with *Listeria monocytogenes* and survival was monitored daily for 20 days. **b)** Proportion of weight loss. **c,d)** Bacterial loads in the liver and spleen on day 1. **e,f)** Bacterial loads in the liver and spleen on day 3. **g)** Livers were collected on day 3 and immunohistochemistry was performed for *L. monocytogenes* using anti-*Listeria* antibody. Arrows indicate the presence of *L. monocytogenes* in the WT liver section. **h)** Livers from *L. monocytogenes* infected mice showing inflammatory lesions indicated by arrows. **i,j)** WT and *Nlrp6*$^{-/-}$ mice were infected i.p. with *Salmonella typhimurium*. Bacterial loads were determined in the liver and spleen on day 1. **k,l)** Bacterial loads in the liver and spleen on day 3. Each point represents an individual mouse, and the line represents the mean ± s.e.m; p values were determined by an unpaired two-tailed test. Results show cumulative data from two different experiments.

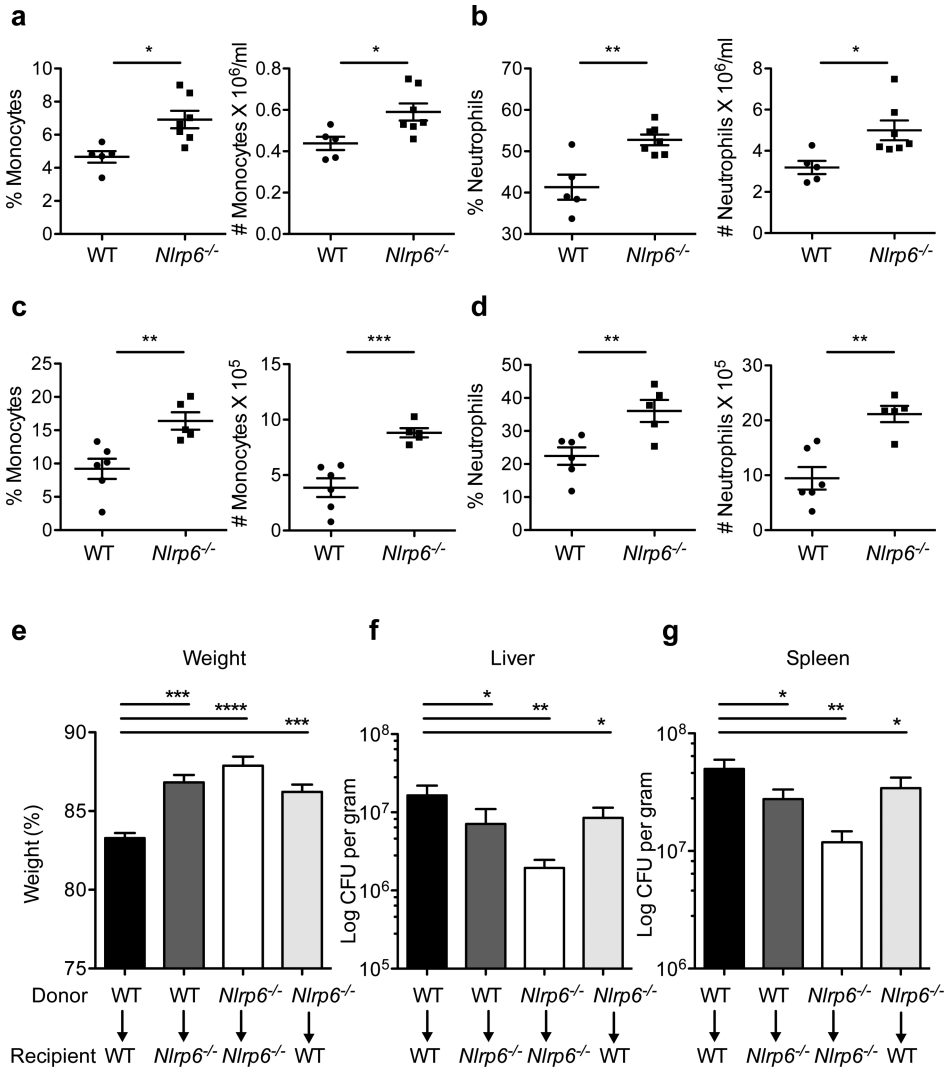

Figure 2. Enhanced monocyte and neutrophil recruitment in infected *Nlrp6*$^{-/-}$ mice

a,b) WT and *Nlrp6*$^{-/-}$ mice were infected i.p. with *L. monocytogenes*. Blood was analyzed for different cell populations based on their morphology. **c,d)** At 6h post-infection, peritoneal lavage was performed on mice infected as above and the cells collected were stained for CD11b^{+}Gr1^{-} (monocytes) and CD11b^{+}Gr1^{+} (neutrophils) cells. **e)** Bone-marrow chimera mice were generated for *Nlrp6* as described in methods. Bar graph shows the percent of weight loss in four groups of chimeric mice. **f,g)** Different groups of chimeric mice, as indicated in the figure panels, were infected with *L. monocytogenes* and bacterial loads were determined in the liver and spleen on day 3. Data show mean ± s.e.m. of a representative experiment.

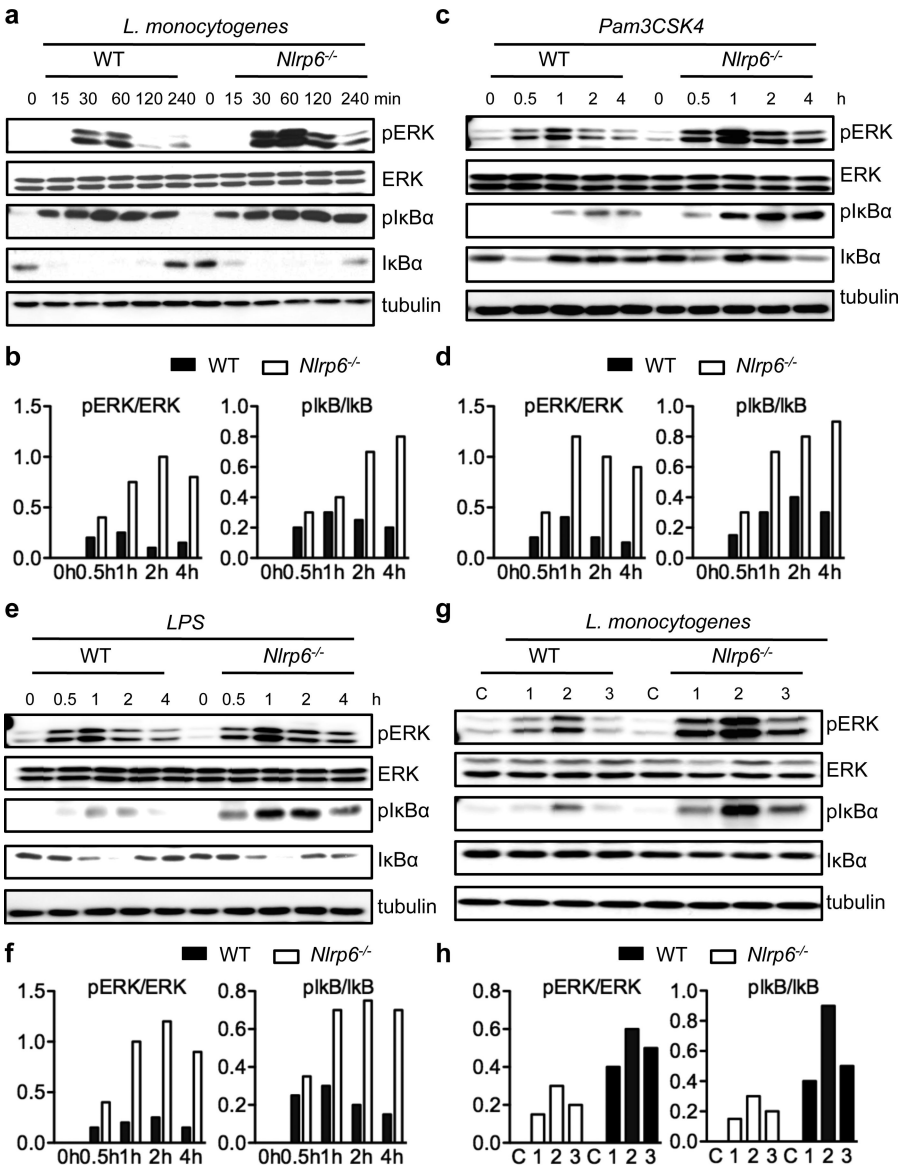

Figure 3. NLRP6 negatively regulates NF-κB and ERK signaling

a,c,e) WT and *Nlrp6*$^{-/-}$ macrophages were exposed to *L. monocytogenes* or Pam3 or LPS and samples were immunoblotted with indicated antibodies. **b,d,f)** Bar graphs showing semi-quantitation of pERK and pIκB levels relative to ERK and IκB levels. **g)** Liver lysates from WT and *Nlrp6*$^{-/-}$ mice were examined for activation of NF-κB and MAP-kinase signaling by Western blot analysis. Each lane represents an individual mouse. **h)** Bar graphs showing semi-quantitation of pERK and pIκB levels relative to ERK and IκB levels, respectively.

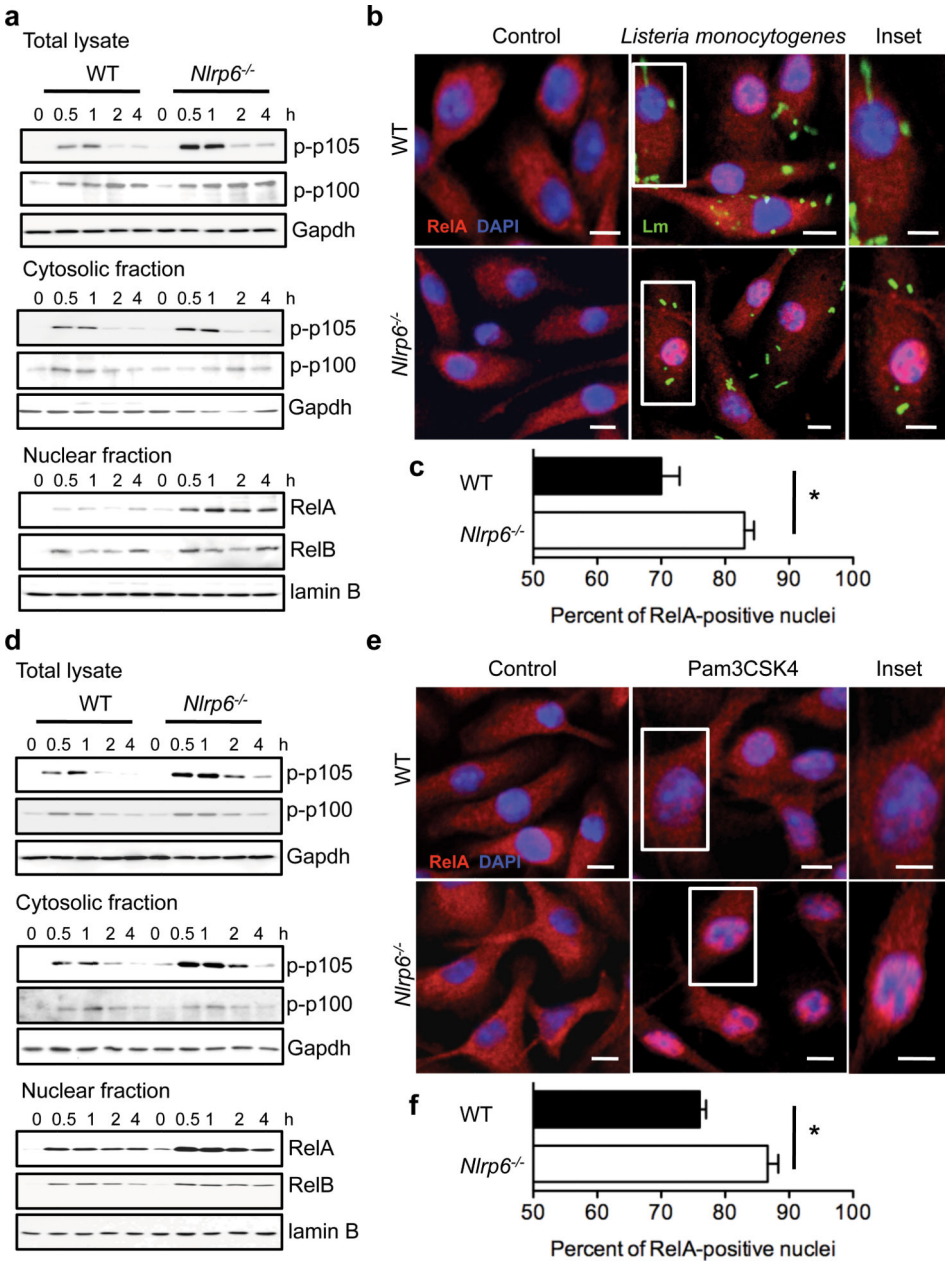

Figure 4. NLRP6 negatively regulates canonical NF-κB activation pathway

a) Bone-marrow derived macrophages from WT and *Nlrp6*$^{-/-}$ mice were infected with *L. monocytogenes* and phosphorylation of p105 and p100 was examined in total cell lysate and cytosolic fraction. Nuclear fraction was examined for RelA and RelB activation in WT and *Nlrp6*$^{-/-}$ cells. **b)** Cells grown on coverslips were infected with GFP-labeled *L. monocytogenes* and examined for nuclear translocation of RelA using anti-RelA antibody (red). Scale bars, 10μm **c)** Quantitative analysis of RelA-positive nuclei is shown. **d)** WT and *Nlrp6*$^{-/-}$ macrophages were stimulated with Pam3 and phosphorylation of p105 and p100 was examined in total cell lysate and cytosolic fraction. Nuclear fraction was examined for RelA and RelB activation in WT and *Nlrp6*$^{-/-}$ cells. **e)** Cells grown on coverslips were stimulated with Pam3 and examined for nuclear translocation of RelA using anti-RelA

antibody (red). Scale bars, 10μm **f)** Quantitative analysis of RelA-positive nuclei is shown. Data show mean ± s.e.m. from three different experiments.